Control of the radial electric field shear by modification of the magnetic field configuration in LHD

K.Ida† M.Yoshinuma† M.Yokoyama† S.Inagaki† N.Tamura† B.J.Peterson† T.Morisaki† S.Masuzaki† A.Komori† Y.Nagayama† K.Tanaka† K.Nariharа† K.Y.Watanabe† C.D.Beidler‡ LHD experimental group

† National Institute for Fusion Sciences, Toki, Gifu 509-5292, Japan
‡ Max-Planck Institut fuer Plasmaphysik, Greifswald D-17491, Germany

Abstract. Control of the radial electric field, E_r, is considered to be important in helical plasmas, because the radial electric field and its shear are expected to reduce neoclassical and anomalous transport, respectively. In general, the radial electric field can be controlled by changing the collisionality, and positive or negative electric field have been obtained by decreasing or increasing the electron density,respectively. Although the sign of the radial electric field can be controlled by changing the collisionality, modification of the magnetic field is required to achieve further control of the radial electric field, especially producing a strong radial electric field shear. In the Large Helical Device (LHD) the radial electric field profiles are shown to be controlled by the modification of the magnetic field by 1) changing the radial profile of the helical ripples, ε_h, 2) creating a magnetic island with an external perturbation field coil and 3) changing the local island divertor coil current.

PACS numbers: 52.55.Hc, 52.50.Sw, 52.50.Gj

1. Introduction

Since the radial electric field and its shear was recognized to play an important role on the improvement of transport, the control of the radial profile of the radial electric field is one of the important tools to improve confinement in toroidal plasmas. In tokamak plasmas, the transition of the radial electric field is observed to be associated with the transition from L-mode to H-mode plasma[1, 2]. In stellarator and Heliotron plasmas, the transition of the radial electric field is triggered by the neo-classical non-ambipolar ion and electron flux, and the radial electric field becomes positive (in the electron root) when the plasma collisionality is low enough, while it is negative (in the ion root) at higher collisionality. Associated with transition of radial electric field from negative (ion root) to large positive (electron root), the reduction of electron thermal diffusivity is observed in CHS, Wendelstein-7AS and LHD plasmas[3, 4, 5, 6, 7] Therefore

it is important to investigate the technique to control radial electric field profiles and understand the physics behind them. In this paper, the control of the radial electric field profiles and the effect of radial electric field on transport especially particle/impurity transport are described.

2. Control of Radial electric field

The Large Helical Device (LHD) is a Heliotron device (poloidal period number L = 2, and toroidal period number M = 10) with a major radius of R_{ax} =3.5 - 4.1 m, an average minor radius of 0.6 m, magnetic field up to 3T , and heating neutral beam with negative ions with a beam energy of 150 - 180 keV. Typically two-thirds of the total beam energy is deposited to the electrons, because of this high beam energy. The radial electric field (E_r) is derived from the poloidal and toroidal rotation velocity and pressure gradient of Neon impurity measured with charge exchange spectroscopy[8] at the mid plane in LHD (vertically elongated cross section) using radial force balance. The radial force balance equation can be expressed as $E_r = (en_I Z_I) - 1(dp_I/dr) - (v_\theta B_\phi - v_\phi B_\theta)$, where B_ϕ and B_θ are the toroidal and poloidal magnetic field and Z_I, n_I, p_I are the ion charge, density and pressure of the measured impurity, respectively. The Large Helical Device (LHD) has n/m=1/1 external perturbation coils. The size of the bmagnetic island can be controlled up to 10cm by changing the current of the perturbation coils. The spatial resolution of the measurements of the radial electric field using the charge exchange spectroscopy is determined by the length of integration of the signal along the line of sight within the beam width of the neutral beam. The spatial resolution becomes poor near the plasma center and relatively good near the plasma edge and it is +/- 1.5cm at the R=4.05m. In this experiment, radial profiles of electron density are measured with FIR and CO2 laser interferometers, while the electron temperature profiles are measured with a YAG Thomson scattering system and ion temperature profiles are measured with charge exchange spectroscopy. The total radiation power is measured with a bolometer.

2.1. Helical ripple strength

Since the radial electric field in LHD is determined by the ambipolar condition of ion flux and electron flux that are trapped in the helical ripples, a change in the magnitude and radial profiles of helical ripples will be the most straightforward tool to control the radial electric field[9]. In LHD, the radial profiles of helical ripples can be modified by a shift of the magnetic axis from 3.5m to 3.9m as seen in Fig.1.

Figure 2 shows the radial profiles of the radial electric field for the ion root (large neoclassical flux with negative E_r in the high collisionality regime), electron root (small neoclassical flux with positive Er in the low collisionality regime) and the transition regime (between ion root and electron root) for various configurations with different helical ripple profiles. When the helical ripple increases gradually towards the plasma edge (R_{ax}=3.75m, 3.9m), the electron root region extends to half of the plasma minor

radius and the radial electric field shear produced is relatively weak. However, when the helical ripple increases sharply at the plasma edge (Rax=3.5m), the electron root region is localized at the plasma edge and strong radial electric field shear is produced. When the magnitude of the helical ripple is suppressed to a low level (R_{ax}=3.6m), the transition region of the radial electric field is located at $\rho = 0.9$, not at the plasma edge, because there is no increase in the helical ripple at the plasma edge in this configuration. These results show that a strong magnetic field shear can be obtained at the plasma edge by shifting the magnetic axis inward rather than shifting the magnetic axis outward, where the achievement of electron root itself is relatively easy (even with higher collisionality).

The measured radial profile of the radial electric field is consistent with that estimated from neoclassical calculation. Figure 3 shows the radial profiles of electric field estimated with the neoclassical calculation using the model profile of temperature and density. Two examples of radial electric field are presented, one is a radial electric field profile in the electron root plasma with low density and the other is a radial electric field profile in the ion root plasma with high density. The transition between electron root and ion root is localized near the plasma edge ($\rho > 0.8$) for the plasma with magnetic axis of 3.5m, while it is located in the plasma core ($\rho < 0.8$) for the plasmas with magnetic axes of 3.6, 3.75 and 3.9m. The difference in the radial profile of the radial electric field is due to the difference in the radial profile of the helical ripple.

The electron density at the transition from ion root to electron root is 0.7 x $10x^{19}m^{-3}$ for the plasma with the magnetic axis of 3.5m, while it is 1.3 x $10x^{19}m^{-3}$ for the plasma with the magnetic axis of 3.9m. The difference in critical electron density can be explained by the differences in the magnitudes of the helical ripples. As seen in Fig.4, the transition from ion root to electron root occurs when the collisionality normalized by the bounce frequency of helically trapped particles decreases below 0.1, which is consistent with the prediction by neoclassical theory[10, 11]. In the plasmas with large helical ripples (R_{ax}=3.75m, 3.9m), a reduction of the thermal diffusivity is observed associated with the transition from the ion root to the electron root. However, there is no reduction of the thermal diffusivity observed associated with the transition in the plasma with small ripples (R_{ax}=3.5m, 3.6m), because neoclassical transport is always smaller than anomalous transport.

2.2. Magnetic island

Formation of the magnetic island is considered to be a useful tool to produce strong radial electric field shear at the boundary of the magnetic island, since the plasma flow is expected to be damped inside the magnetic island. The size of the magnetic island in the plasma is normally smaller than that expected by the vacuum magnetic field because the healing effect[12]. This healing effect becomes larger in the plasma with lower collisionality[13, 14]. The island structure of the radial electric field was investigated for the medium density plasma in the ion root and radial electric field shear is observed at the boundary of the magnetic island[15]. This raised the question as to whether radial

electric field shear can be produced in the electron root plasma, where the collisionality might be too low to produce a magnetic island. Figure 5(a) show the radial electric field profiles for various currents of the n/m=1/1 external coils for the electron root. When the n/m=1/1 perturbation field due to LID current is small enough there is no magnetic island structure observed. As the perturbation field is increased, a clear magnetic island structure appears in the radial profiles of the radial electric field. The radial electric field becomes zero at the magnetic island (R= 4.00m - 4.08m). Relatively large radial electric field shear is produced at both boundaries of the magnetic island. As shown in Fig.5(b), there is no magnetic island observed at normalized LID currents less than 250A/T, because of the healing of the magnetic island. However, when the normalized LID current exceeds 300A/T, the magnetic island suddenly appears and the size of the magnetic island jumps to close to that expected from the calculated vacuum magnetic flux surface. The location of the magnetic island (center of magnetic island at the mid-plane) moves inside when the n/m=1/1 perturbation field becomes strong as shown in Fig5(c). When the size of the magnetic island is large, the location of the center of the magnetic island is consistent with that expected from vacuum magnetic flux surfaces. However, the location of the magnetic island moves to the inner side as the LID current is increased, although the LID current does not affect the location of the magnetic island in vacuum as seen in Fig.5(b) The shift of location of the magnetic island is observed in the electron root plasma but not in the ion root plasma[15].

Because the radial electric field shear may exist at the boundary of the magnetic island, the transport barrier may start near the boundary of magnetic island. In fact the magnetic island contributes to the formation of an electron internal transport barrier (ITB) near the threshold power of ECH for the transition to ITB in LHD[16]. Therefore it is considered that the magnetic island may contribute to the formation of the ion internal transport barrier, which has not been observed in LHD yet. The radial electric field itself is expected to affect the particle transport especially impurity transport[17, 18, 19], which is in contrast to the radial electric field shear effect on the energy transport. In the CHS experiment, the impurities tend to accumulate at the plasma axis and the impurity and electron density profiles tend to peaked in plasmas with negative electric field, while the impurity is exhausted and impurity and density profiles are hollow in plasmas with positive electric field[20]. Therefore it is expected that the positive electric field should contribute to suppress the influx of impurities and prevent the radiation collapse.

Figure 6 shows the radial profile of the radial electric field for the plasma in the electron root with a helical divertor (standard configuration) and ion root with a limiter configuration and a Local Island Divertor (LID)[21] configuration, where a part of the magnetic island is connected to the local island divertor head. The measured radial profiles of the radial electric field are consistent with those estimated by neoclassical calculation for the electron root plasma with the helical divertor and ion root plasma with a limiter configuration. In the divertor (LID) configuration, a large positive electric field with a sharp radial electric field shear is observed, while the radial electric field

is negative for the plasma with a limiter configuration. The sign of the radial electric field changes from negative to positive by crossing the X-point of the magnetic island. This positive electric field is considered to be produced by the electron loss along the magnetic field line toward the LID limiter head. The radial electric field estimated from neoclassical theory becomes more negative towards the plasma edge, while the radial electric field measured becomes positive towards the plasma edge. There is a large discrepancy in radial electric field between the measurements and neoclassical prediction near the X-point, because the electron loss along the magnetic field line is not included in the neoclassical calculation. Since this positive electric field is located in the region of the direct electron loss, the radial electric field shear in this region could not contribute to the improvement of the electron transport. However, the radial electric field at the edge plays a role in preventing the influx of impurities into the plasma with an LID configuration.

3. Role of Radial electric field on impurity transport

The role of positive radial electric field in preventing the impurity influx is observed in experiments in the plasma with radiation collapse. When the short Ne puff is applied to the plasma in the early phase of the discharge, there are two type of discharges; one is a steady state discharge without radiative collapse, the other is a transient discharge resulting in radiative collapse even when the Ne puff is already turned off [Fig7(a)]. The 10 % increase of Ne puff (from 180ms pulse width to 200ms pulse width) early in the discharge causes this difference. Therefore there should be a feedback mechanism in the radiation collapse related to the increase of the electron density. The temperature dependence of the cooling coefficient results in the sharp increase of radiation power proportional to n_e^3[22]. However the spontaneous gradual increase of radiation power proportional to n_e^1 well before the radiation collapse(t = 0.8 - 1.4sec). can not e explained by increase of cooling rate. There should be a feedback mechanism relating particle and/or impurity transport and radial electric field. As seen in Fig.7, the radial electric field starts to be more negative 0.5 sec before the radiative collapse. The radial electric field becomes more and more negative until the radiative collapse. The change of radial electric field to more negative is due to the increase of the collisionality (increase of electron density and decrease of temperature). When the radial electric field becomes more negative, the negative radial electric field causes an increase of the impurity influx, because the exhausting effect by positive radial electric field disappears. In the discharge without radiation collapse, the radial electric field remains positive with no increase of the electron density and radiation power. The ion temperature shows a significant drop down to 150eV just before the radiation collapse. Associated with decreasing temperature, the NeX intensity also drops because the fully ionized neon decreases by the recombination process. These drops are not observed in the discharge without radiation collapse. These data shows there are two steps in the discharge towards the radiative collapse. Until just before the radiative collapse (t $<$ 1.27 sec), there is no

significant drop of temperature. Negative electric field causes the increase of density and the radial electric field becomes more negative due to the increase of collisionality. This feedback process between the negative radial electric field and the increasing electron density should be the most important process. Just before the radiation collapse (t > 1.27 sec), the feedback process between the decreasing temperature and increasing cooling rate also is considered to be important.

Figure 8(a)(b) show the time slice of the radial electric field and the ion temperature in the discharge, which is terminated by radiative collapse. The negative electric field is localized near the plasma edge at r = 0.8 - 0.9. Just before the radiative collapse (t = 1.43 sec), the negative radial electric field region extends to more inside of the plasma (ρ < 0.7 - 0.8) and the edge radial electric field becomes less negative at t = 1.42s. Although the negative electric field is localized in the narrow region ($\delta\rho$ = 0.1), the drop of ion temperature is observed in the wide region. The decrease of intensity of the charge exchange line of NeX just before the radiation collapse is due to the recombination of fully ionized Neon associated with the drop of the electron temperature. These observations show that the positive electric field is quite important to avoid the radiation collapse and are consistent with the experimental results in the LID configuration, where the impurity influx is shielded by the strong positive electric field near the X point of the magnetic island[23].

4. Discussions

The strong shear of the radial electric field is demonstrated to be produced inside the plasma by controlling the helical ripple and the magnetic topology (magnetic island and LID configuration) to trigger an internal transport barrier and reduce impurity influx. The radial electric field shear is demonstrated to be controlled by the modification of the helical ripple associated with the shift of the magnetic axis, while the sign of the radial electric field is controlled by the collisionality. The magnetic configuration with a sharp gradient in the helical ripple is considered to be more appropriate for creating the strong radial electric field shear. The magnetic island produces the radial electric field shear at the boundaries of the magnetic island and hence contributes to trigger the formation of an internal transport barrier in the electron root plasma. The transient improvement of the ion transport in the ion root is also observed after the pellet injection with the assistance of n/m=1/1 island. This is due to the fact that the increase of the electron density gradient by pellet injection is transient and there is not enough particle source to sustain the density gradient. This improvement is expected to be sustained in the steady state by increasing ion heating power and beam fueling using a low energy beam of 40 keV, which is planned to be installed in LHD in the near future to increase the heating power to ions. In addition to the temperature dependence of the cooling rate, the feedback mechanism in which negative electric field causes an increase of the density, which results in a more negative electric field, is crucial to the process of radiative collapse. The role of radial electric field is found to be quite important to prevent the

influx of impurities and avoid the radiative collapse. The positive electric field observed in the LID configuration is considered to play an important role for impurity shielding. Therefore the improvement of thermal transport and impurity exhaust are achieved by the control of radial electric field profiles in LHD.

The authors would like to thank the LHD technical staff for their effort to support the experiments in LHD. This work is partly supported by a grant-in-aid for scientific research of MEXT Japan.

References

[1] R.J.Groebner, K.H.Burrell, and R.P.Seraydarian, Phys. Rev. Lett. 64, (1990) 3015
[2] K.Ida, et. al., Phys Rev Lett 65 (1990) 1364.
[3] A.Fujisawa, et. al., Phys Rev Lett 82 (1999) 2669.
[4] U.Stroth, et. al., Phys Rev Lett 86 (2001) 5910.
[5] T.Shimozuma et al., Plasma Phys Control Fusion 45 (2003) 1183.
[6] K.Ida, et. al., Phys Rev Lett 91 (2003) 085003.
[7] Y.Takeiri et al., Phys. Plasma 10 (2003) 1788
[8] K.Ida, S. Kado, Y. Liang, Rev. Sci. Instrum. 71 (2000) 2360.
[9] K.Ida, et. al., Phys Rev Lett 86 (2001) 5297.
[10] C.D.Beidler et al., Plasma Physc. Controll. Fusion 36 (1994)317
[11] M.Yokoyama, et al., Nucl. Fusion 42 (2002) 143.
[12] K.Narihara, et al., Phys Rev Lett 87 (2001) 35002
[13] N.Ohyabu et al., Phys Rev Lett 88 (2002) 55005
[14] Y.Nagayama et al., submitted to Nucl. Fuion.
[15] K.Ida, et al., Phys Rev Lett 88 (2002) 015002.
[16] K.Ida, et. al., Phys plasmas 11 (2004) 2551.
[17] K.Ida, et. al., Phys Rev Lett 68 (1992) 182.
[18] Y.Nakamura, et. al., Nucl Fusion 43 (2003) 219.
[19] K.Ida, et. al., Plasma Phys Control Fusion 45 (2003) 1931.
[20] K.Ida et. al., Phys Plasmas 08 (2001) 1.
[21] A.Komori et al., submitted to Nucl. Fuion.
[22] B.J.Peterson et al., submitted to Nucl. Fuion.
[23] T.Morisaki et al., J. Nucl. Mater to be pubulished

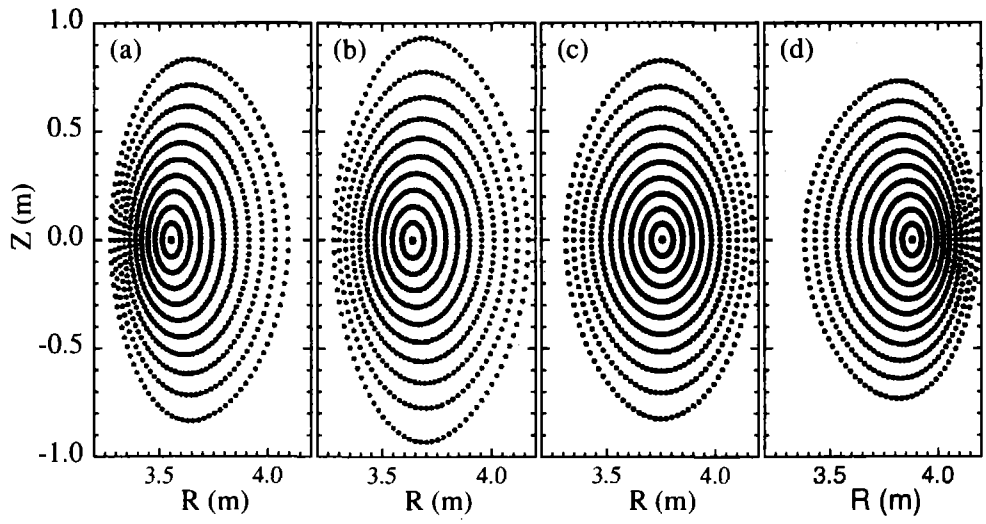

Figure 1. (a)Poloidal cross section of the magnetic flux surface for plasmas with various magnetic axis, R_{ax} of(a)3.5m, (b)3.6m, (c)3.75m, and (d)3.9m.

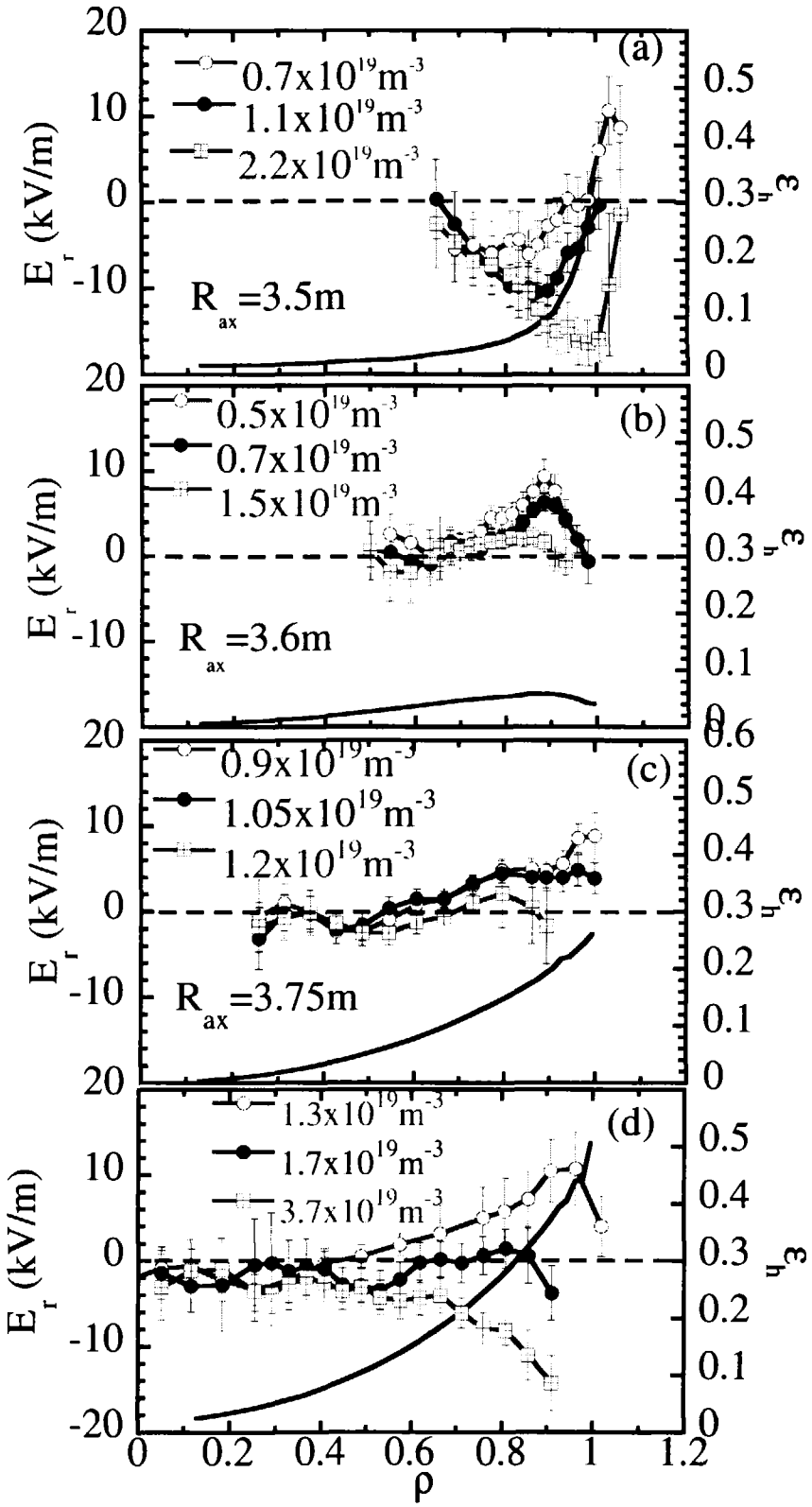

Figure 2. Radial profiles of radial electric field, Er and helical ripple ϵ_h for plasmas with various magnetic axis, R_{ax} of (a)3.5m, (b)3.6m, (c)3.75m, and (d)3.9m.

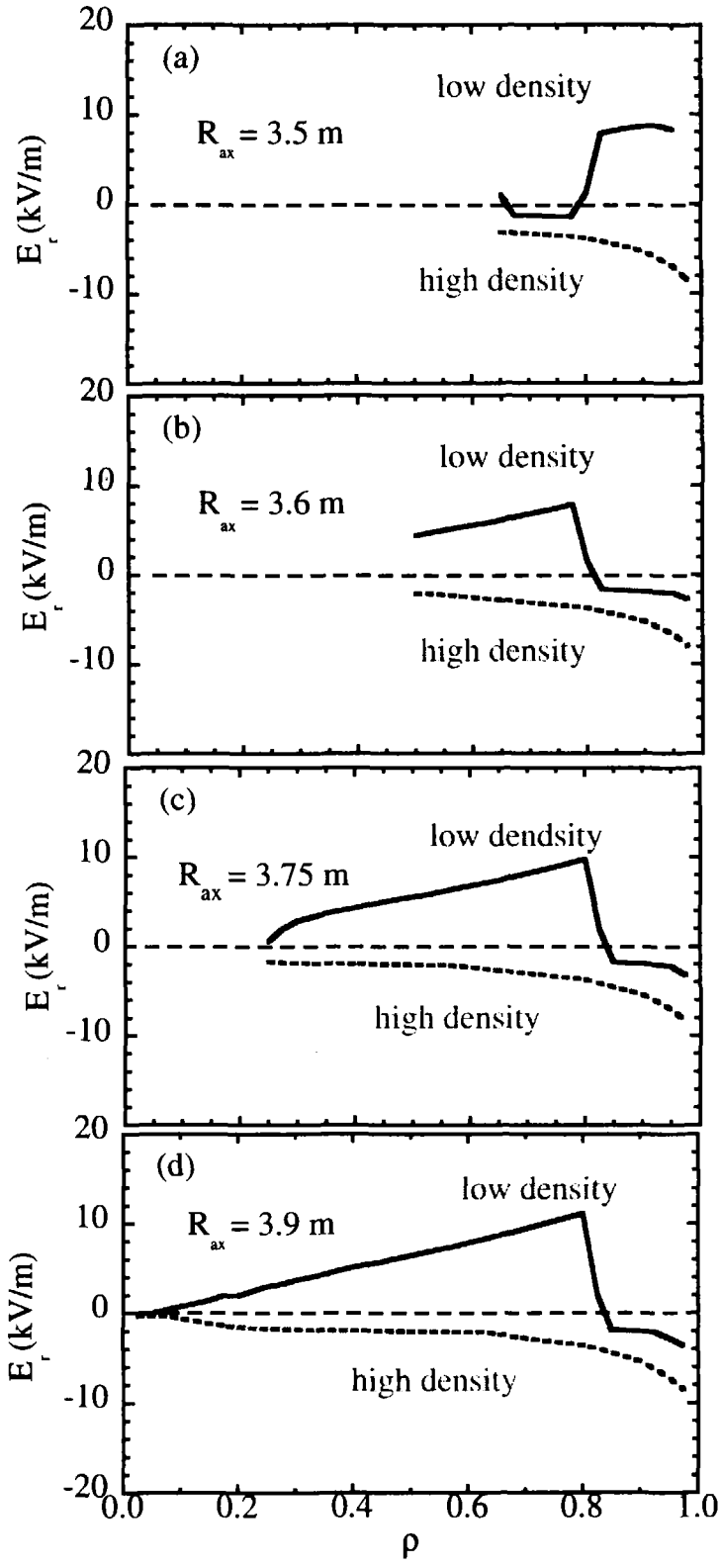

Figure 3. Radial profiles of radial electric field, Er calculated with NC theory for plasmas with various magnetic axis, R_{ax} of (a)3.5m, (b)3.6m, (c)3.75m, and (d)3.9m.

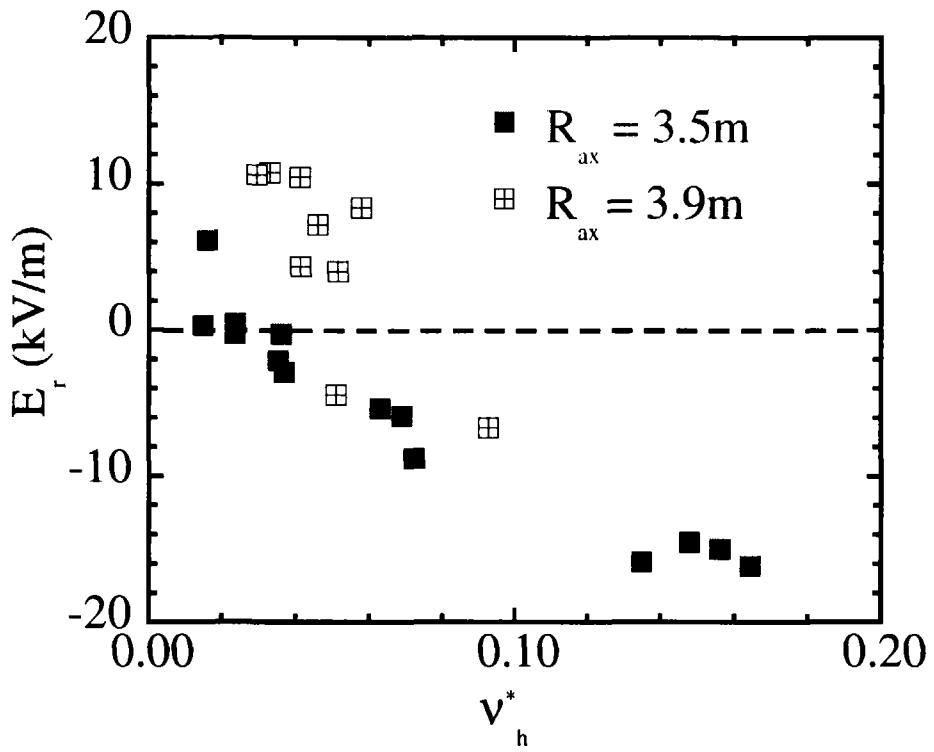

Figure 4. Radial electric field as a function of collisionality normalized by the bounce frequency of helically trapped particles.

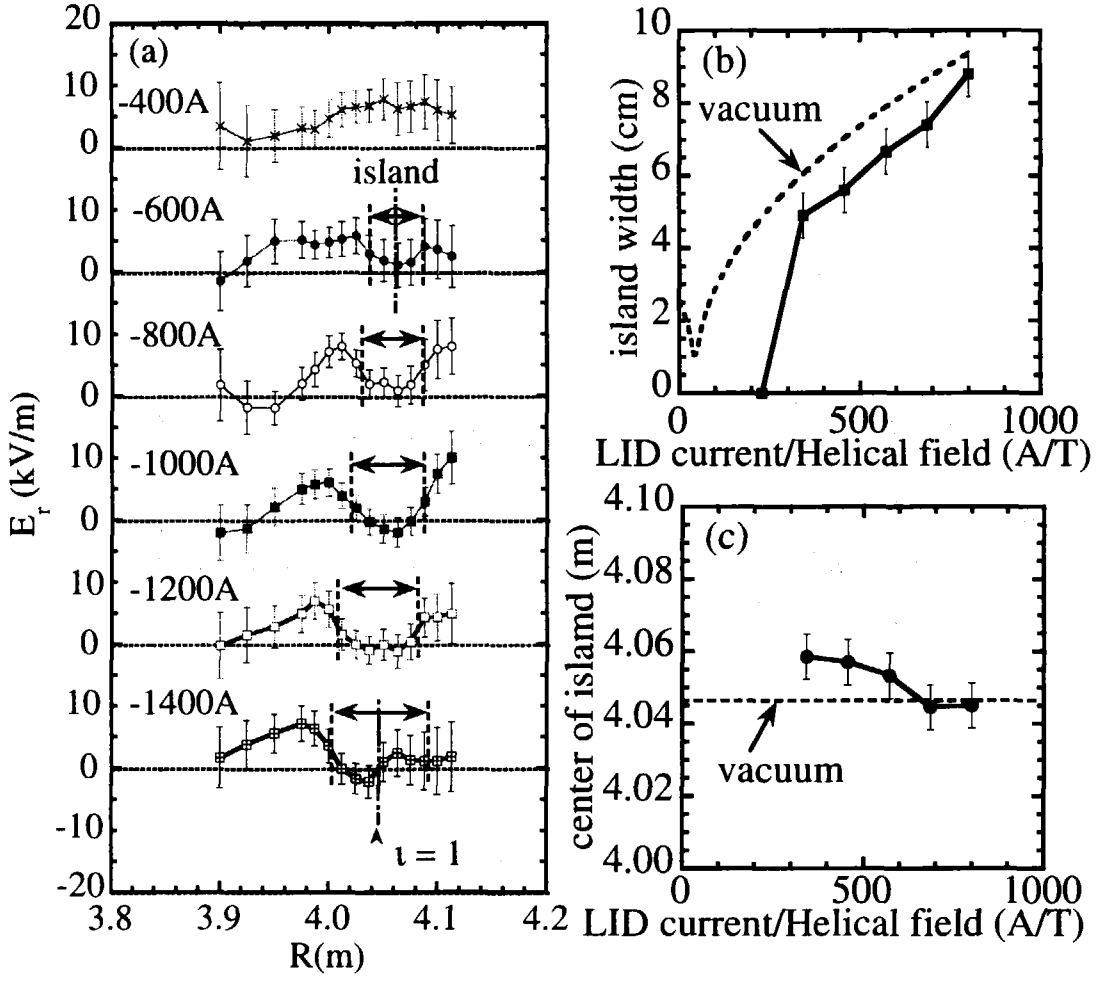

Figure 5. (a)Radial profiles of radial electric field with magnetic island for the plasma in the electron root (b) width of magnetic island at the mid-plane and (c) position of center of magnetic island as a function of LID perturbation field normalized by helical magnetic field.

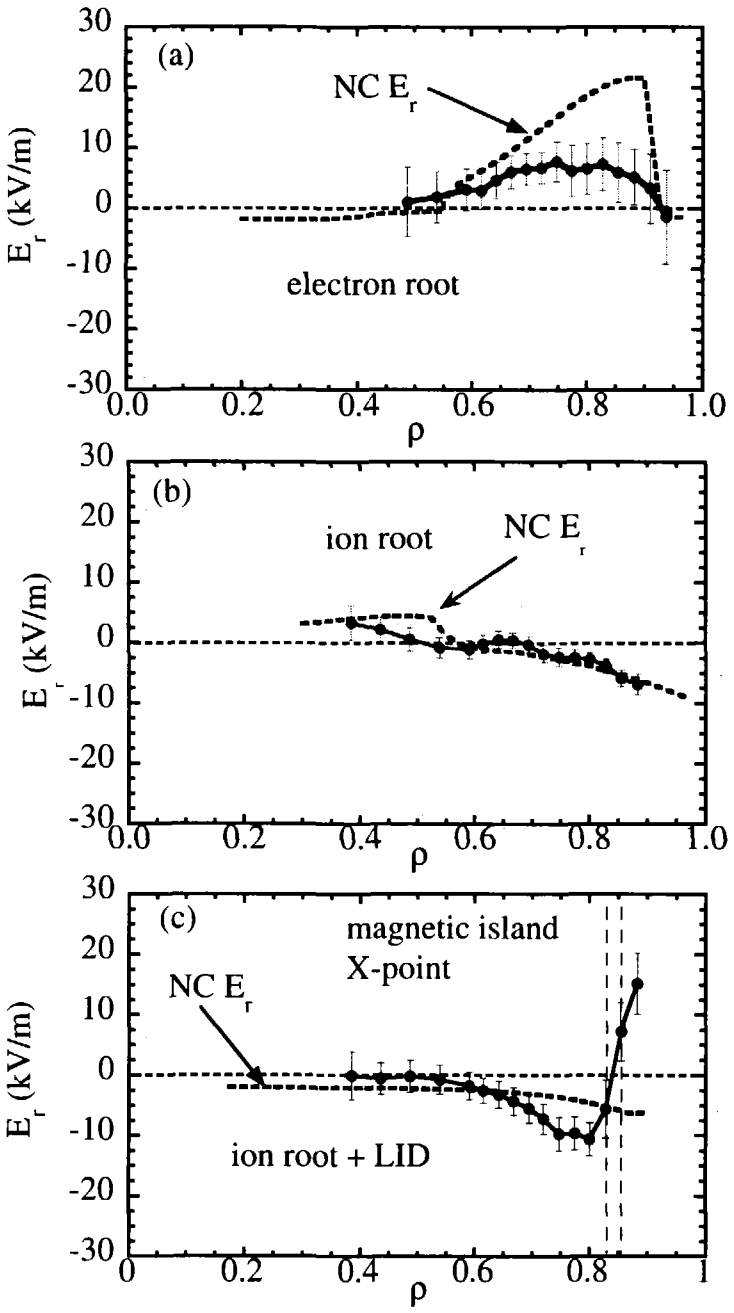

Figure 6. Radial profiles of radial electric field measured and neoclassical prediction (dotted lines) for the plasmas (a) in the electron root (b) ion root in limiter configuration and (c) ion root with a local island divertor configuration.

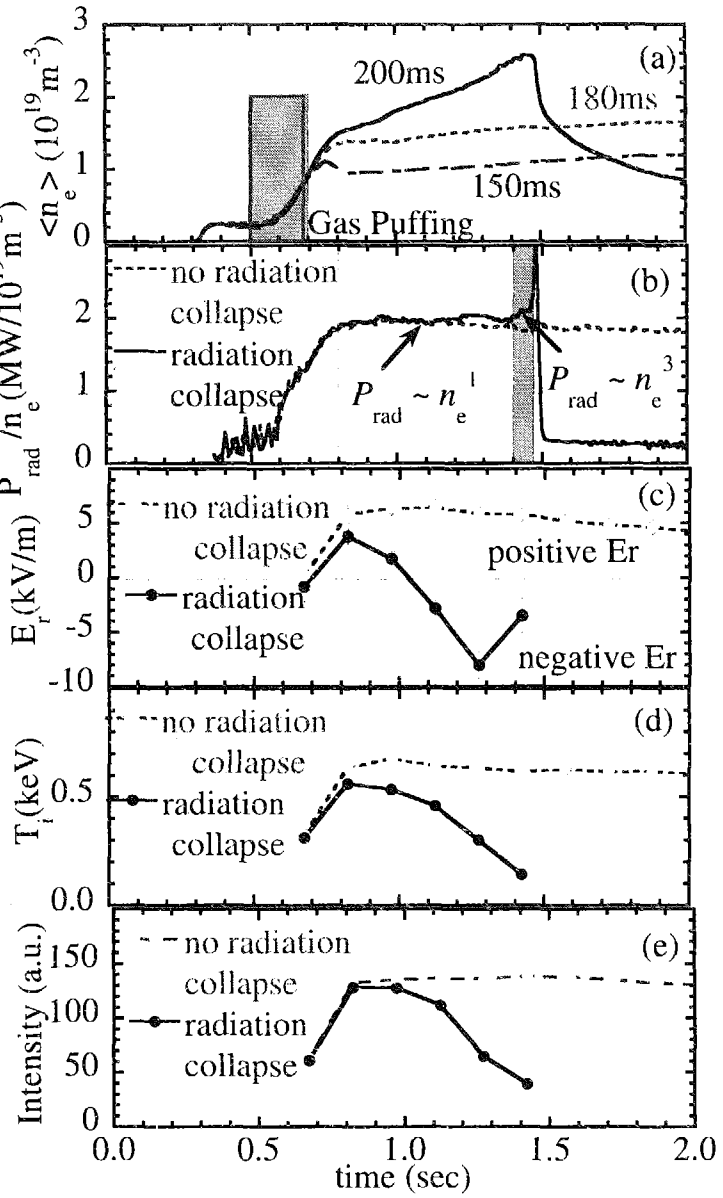

Figure 7. Time evolution of (a) line averaged electron density (b) normalized total radiation power (c) radial electric field (d) ion temperature and (e) NeX intensity at $\rho = 0.89$ for the discharges with and without radiation collapse.

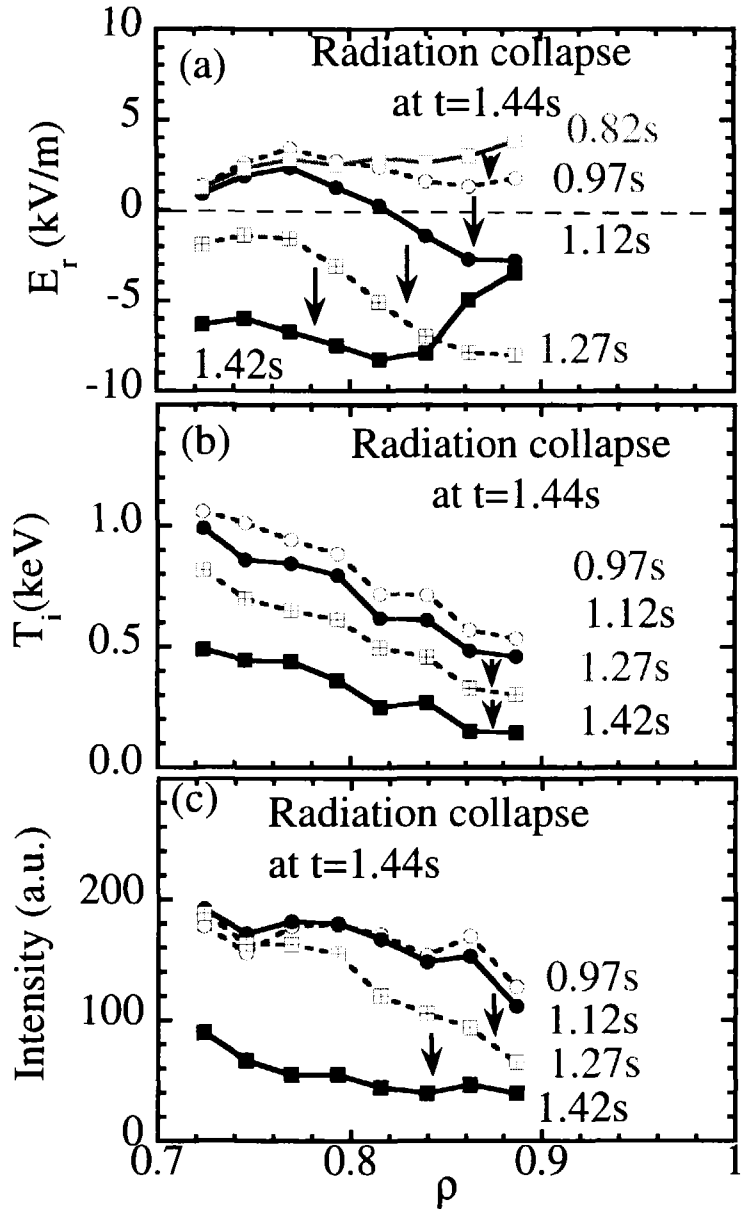

Figure 8. Radial profiles of (a) radial electric field, (b) ion temperature and (c) intensity of charge exchange line NeX in the discharges with radiation collapse.